

Thermal Conductivity of Solid Hydrogen*

R. G. Bohn[†] and C. F. Mate

Department of Physics, Ohio State University, Columbus, Ohio 43210

(Received 15 September 1969)

The thermal conductivity of solid parahydrogen containing 0.2 to 5% orthohydrogen has been measured over the temperature range 1.5–6°K. On the low-temperature side of the conductivity maximum, the conductivity shows both a T^3 dependence and a strong dependence on orthohydrogen concentration. Within the resolution of the measurements, no (static) impurity scattering attributable to the orthohydrogen could be detected. We discuss the significance of these results in relation to a recent calculation that emphasizes the impurity scattering of phonons by orthohydrogen.

I. INTRODUCTION

Measurements of the thermal conductivity of solid hydrogen with orthohydrogen concentrations from 0.5 to 72% were reported by Hill and Schneidmesser¹ in 1958. They found that the additional thermal resistance produced by adding orthohydrogen showed a T^{-n} temperature dependence, with $2 < n < 3$. It was concluded that phonon scattering at grain boundaries might be responsible for the effects observed, but there seemed to be no reason to expect the grain size to depend on the orthohydrogen concentration. Alternatively, it was pointed out that the additional resistance might be attributable directly to phonon scattering by the orthohydrogen molecules, although no estimate could be given of the expected temperature dependence of the conductivity. In a recent treatment of this problem Ebner and Sung² concluded that the resistive term contributed by phonon-orthohydrogen scattering should vary with temperature approximately as T^{-2} . The measurements described below for orthohydrogen concentrations between 0.2 and 5% extend to lower temperatures than those of Hill and Schneidmesser. At the lowest temperatures they show a thermal resistivity that varies closely as T^{-3} , but with a dependence on orthohydrogen concentration very similar to that predicted by Ebner and Sung.

II. EXPERIMENTAL

Parahydrogen samples with low orthohydrogen concentration (near 0.2%) were prepared by placing liquid hydrogen (5% *o*-H₂) in contact with a chrome alumina catalyst for several hours. After the thermal conductivity of the solid had been measured at this concentration, the sample was stored at room temperature for several days to allow some para-to-ortho conversion to take place before the next set of conductivity measurements. By repetition of this procedure, conductivity measurements were made on one sample at orthohydrogen concentrations of 0.34, 0.52, 1.1, 2.5, and 5.0%, and on a second sample at concentrations of 0.20 and 0.71%.

In each case, the orthohydrogen concentration was measured immediately before or immediately after the conductivity run. For reasons of convenience, the concentration was determined in a separate NMR cryostat by measuring the spin-lattice relaxation time of the solid.³ At the lowest concentrations the precision of this method was probably not better than $\pm 10\%$, but this is adequate for our present purpose.

Figure 1 shows the conductance cell in which the hydrogen crystals were grown for the conductivity measurements. The stainless-steel sample tube (0.010-in. wall) in the cell was connected by a 1-mm filling tube to a storage bulb which was at room temperature. With the He⁴ subpot empty, and with liquid He⁴ at 4.2°K surrounding the Pyrex glass vacuum jacket (containing helium gas at a

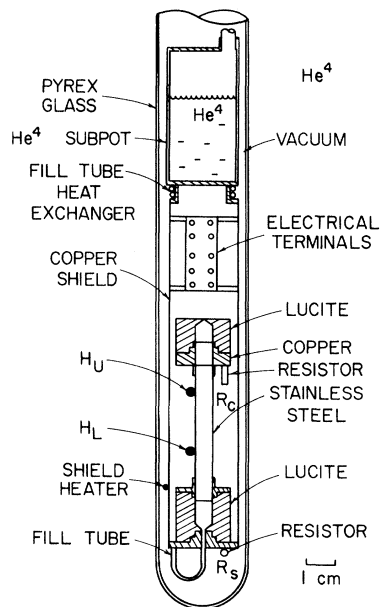


FIG. 1. Diagram of the cell in which crystals were grown for the conductivity measurements.

pressure of less than 1 mTorr), the cell was allowed to cool slowly until the hydrogen sample began to condense into it, at about 20°K. The hydrogen was prevented from solidifying in the filling tube, which runs through the He⁴ bath, by vacuum jacketing the tube and wrapping it with a manganin heating coil. Condensation and cooling continued until the cell was full of liquid near the triple point, then the filling line heater was switched off. When the liquid in the cell had cooled to the triple point, or a little below, the solid phase began to form at the bottom of the sample space, the shape of which was designed to encourage the nucleation and growth of a single crystal. The growing crystal was observed through the lucite wall of the lower part of the sample space and its rate of growth was controlled by adjusting the temperature gradient in the liquid with the upper heater (H_U) on the conductance cell.

As the liquid solidified, its decrease in volume produced a small vapor-filled space at the top of the cell. Since the temperature was a little higher at the top of the cell than at the bottom, the temperature and pressure at which the crystal was grown were slightly above the triple-point values. When solidification was complete the temperature fell rapidly from the triple point, reaching 10°K in about 15 min. At this stage, He⁴ was condensed into the subpot and the helium gas that had been used for heat exchange was pumped out of the vacuum jacket. Meanwhile, the sample cooled to 4.2°K. At this temperature the upper end of the crystal was still visible, although it no longer protruded into the upper lucite section of the sample space. The visible parts of the crystal were examined carefully for evidence of cracking or shattering induced by thermal stresses during cooling. The crystal was always clear, as when grown, except for the appearance of a few (rarely more than two or three) threadlike imperfections.

In the thermal-conductivity measurements, a germanium resistance thermometer (R_C, Fig. 1) was used to measure the temperature at the isolated upper end of the conductance cell. A fixed power input was applied first at the lower heater H_L (Fig. 1), then at the upper heater H_U. The measured temperature rise ΔT at the thermometer is due solely to the establishment of the temperature gradient $\Delta T/\Delta X$ (Fig. 2) between the lower and upper heaters when the heat input is switched from one to the other. If the heaters are similarly mounted, and if the distance of each from the heat sink is large compared with the diameter of the sample, this method of determining the temperature gradient provides automatic compensation for end effects and for stray temperature gradients produced by any small constant heat influx (as from

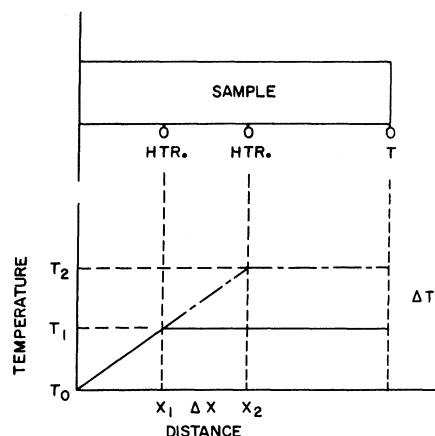


FIG. 2. Schematic of temperature distribution in the sample. Full line is for heat input at H_L; dash-dot line is for the same heat input at H_U. The measured temperature gradient is $\Delta T/\Delta X$.

para-ortho conversion) to the sample. It also offers the considerable advantage of requiring the precise calibration of only one thermometer.

The germanium resistor R_C, encapsulated in He⁴ gas, was mounted in a thermometer well in the copper flange at the top of the sample tube. This flange was also used as a thermal ground for the thermometer leads. In addition, all thermometer and heater leads were thermally grounded both at the copper radiation shield and at the outer He⁴ bath. Since it was important that there should be no temperature drift at the heat sink during a temperature-gradient determination, a second germanium resistance thermometer (R_S, Fig. 1), for which calibration was unnecessary, was mounted at the bottom of the radiation shield for use as a temperature-drift detector. The measured thermal time constant of the conductance cell never exceeded 1 min, so that adequate long-term temperature stability of the heat sink could be achieved by adjustment of the pumping rate at the He⁴ subpot.

With a power dissipation of about 1 μW in the upper thermometer, a resolution of 0.2 m°K in the ΔT measurement could be realized. ΔT itself was typically of order of magnitude 10 m°K for a heater input of 0.1 to 1 mW, depending on the orthohydrogen concentration in the sample. For calibration *in situ* of the thermometer R_C, the vacuum jacket was filled with He⁴ gas and the thermometer resistance was measured at ten temperatures between 1.2 and 4.2°K determined from the vapor pressure⁴ of the outer He⁴ bath. The resistivity ρ of an impurity semiconductor such as *n*-type germanium can be approximated by

$$1/\rho = \sum_{i=1}^n C_i e^{-\epsilon_i/kT}, \quad (1)$$

with perhaps two or three terms necessary for an adequate representation of the low-temperature behavior.⁵ This expression is analytically inconvenient for curve fitting. Moreover, resistivity measurements show small-scale deviations from the smooth temperature variation that it describes.⁶ We chose, therefore, to fit our resistance measurements to a smooth curve of similar shape, namely,

$$Ax^2 + Bxy + Cy^2 + Dx + Ey + F = 0, \quad (2)$$

with $x = 1/T$ and $y = \ln R$. In addition, a deviation curve was constructed from which a correction (never more than 10%) could be applied to each value of $\Delta T (= \Delta R dT/dR)$ computed from Eq. (2). Since an extrapolation of the calibration curve was used for temperature and temperature-difference measurements between 4.2 and 6 °K, we remark that the extrapolation agreed well with the thermometer resistances measured during the condensation and solidification of the hydrogen sample in the conductance cell at temperatures of approximately 19 and 14 °K.

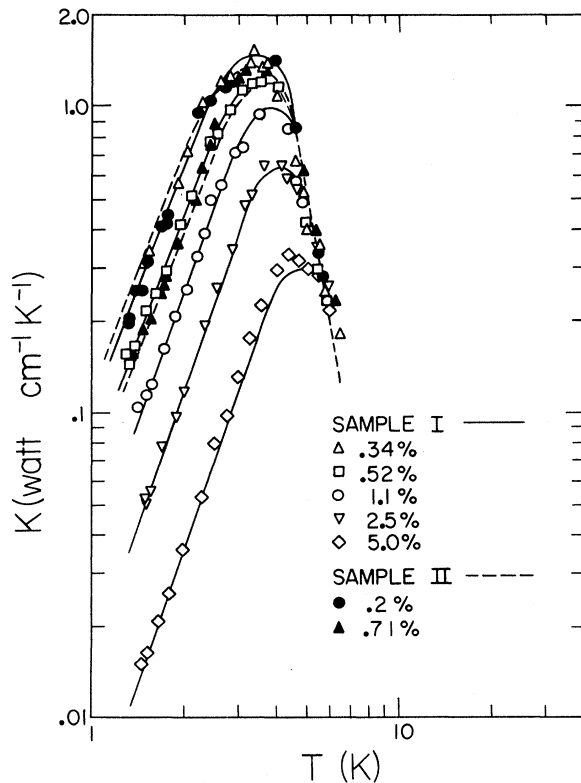


FIG. 3. The thermal conductivity as a function of temperature at several orthohydrogen concentrations. Equation (3) was used to fit the smooth curves to the data.

III. RESULTS AND DISCUSSION

For each orthohydrogen concentration studied, the temperature dependence of the thermal conductivity could be described within the experimental uncertainty by writing its reciprocal $K^{-1}(T)$, the thermal resistivity, as the sum of three terms,

$$K^{-1}(T) = (aT^3)^{-1} + bT + (cT^n e^{\theta/\beta T})^{-1}. \quad (3)$$

Figure 3 shows curves from this expression fitted to the experimental data. We note that, considering the uncertainties in orthohydrogen concentration in both sets of experiments, there is reasonable agreement between these conductivity measurements and those of Hill and Schneidmesser.¹ The general features of the thermal conductivity as exhibited in Fig. 3 are characteristic of dielectric crystals and not of metallic alloys such as the stainless steel of which the sample tube is made. This provides reassurance that the crystal has not been fractured or separated from the wall of the sample tube by the volume strain (approximately 2.5%) introduced when it is cooled from the triple point.

The exponential factor in the Umklapp term of Eq. (3) dominates the high-temperature behavior. Consequently, the data cannot be made to yield any information about the temperature exponent n . And all that can be said about the constant β is that its value is approximately 2. The common curve shown for the high-temperature data was drawn for $n = 3$ and $\beta = 2$, with an approximate value of 109 °K for the Debye temperature Θ_D , taken from the specific-heat data of Hill and Lounasmaa.⁷

The T^3 term, usually regarded as characteristic of boundary scattering, gives an unusually good fit to the data below the conductivity maxima. A least-squares fit to the lower portion of each log-log curve gave slope values, not correlated with the orthohydrogen concentration, ranging from 2.6 to 3.1. The low-temperature portion of each curve in Fig. 3 was drawn with slope 3.0.

Since the height of the conductivity maximum is very sensitive to the presence of small amounts of impurity or other imperfections in the solid, it is to be expected that the Umklapp and boundary-scattering terms alone will fail to give an adequate account of the conductivity in the region of the peak. In fact, for the lowest orthohydrogen concentrations, the combination of these terms gives a peak value approximately 50% greater than the observed maximum conductivity. For this reason, an impurity scattering term bT is included in the expression for the resistivity. Fitting this term to the conductivity maxima, we find that its coefficient b does not depend on the orthohydrogen concentration. The orthohydrogen contribution to the resistivity seems to reside entirely in the "boundary scattering" term.

This is illustrated in Table I, which shows the values obtained for the coefficients a and b at each concentration. The only appreciable change in the coefficient b occurred between the first and second runs with sample II, and we suspect that a small amount of some foreign impurity (e.g., air) was frozen out during the first run and not recovered with the rest of the sample. This might also explain why the conductivity peak for the 0.2% sample is proportionately a little broader than the others, so that Eq. (3) cannot be fitted at the peak without producing a small displacement of the curve from the low-temperature data, as shown in Fig. 3.

The kind of temperature dependence exhibited by the conductivity strongly suggests that a phonon-scattering mechanism independent of phonon wavelength is introduced by the orthohydrogen molecules. The phonon mean free path λ associated with this scattering mechanism is shown as a function of the orthohydrogen concentration in Fig. 4. The expressions

$$K = \frac{1}{3} \lambda_0 C_V v \quad (4)$$

$$1/\lambda_0 = 1/L + 1/\lambda \quad (5)$$

were used to define λ in terms of the low-temperature conductivity (K), the constant-volume heat capacity (C_V), the velocity of sound (v), and a boundary scattering free path (L), assumed equal to the sample diameter. According to Fig. 4, the mean free path is quite closely proportional to the reciprocal of the concentration, except for $x > 2\%$ where the dependence becomes somewhat faster, and at very low concentrations where λ seems to approach a constant value equal to about one-tenth the sample diameter (which was 6 mm). The evidence for this last observation is stronger than Fig. 4 indicates, since the cited value of 0.2% is probably an upper limit for the lowest concentration represented in the figure, and for this sample, λ has almost certainly been overestimated by the curve-fitting difficulties mentioned in the preceding paragraph.

The nature of the scattering mechanism introduced by the orthohydrogen molecules is by no means

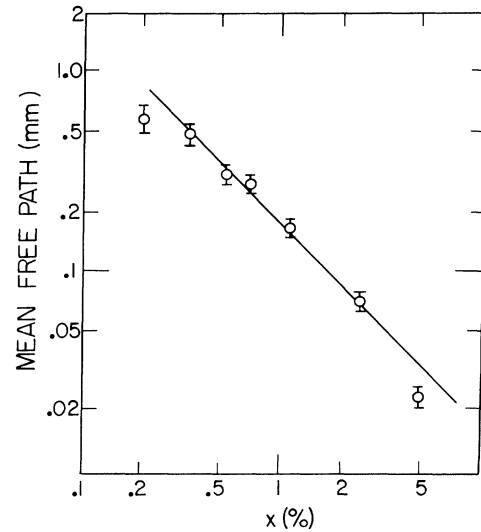


FIG. 4. Phonon mean free path in the T^3 region, as a function of orthohydrogen concentration x . Full line represents $\lambda \propto 1/x$.

obvious. One might suppose, for instance, that they behave as impurities that segregate at grain boundaries when the crystal is grown, producing a total grain boundary area proportional to the orthohydrogen concentration. Then, scattering at the grain boundaries should give a phonon mean free path inversely proportional to concentration, and independent of temperature, as observed. Moreover, if the grain diameter were at all comparable with the apparent mean free path, it would be necessary for only a small fraction of the orthohydrogen molecules to be associated with the boundary substructure.

Any explanation of this kind, however, rests on the assumption that an orthohydrogen molecule is very foreign to the hcp parahydrogen lattice. This contention is difficult to support. Hill and Schneidmeyer¹ pointed out that the density of the solid seems to be nearly independent of orthohydrogen concentration and, in fact, Jarvis, Ramm, and Meyer⁸ have found that for the hcp solid at 4.2°K the density of orthohydrogen is only about 1.3% greater than that of parahydrogen. Hill and Schneidmeyer also observed changes in the conductivity (attributed to ortho-para conversion) that could not be associated with the self-annealing of crystal defects. We remark, in addition, that the orthohydrogen does not seem to contribute to the impurity scattering term in Eq. (3), as it would if point defects were being introduced into the crystal, and that the NMR studies of Harris *et al.*⁹ and of Amstutz *et al.*¹⁰ indicate that the extent to which clusters of orthohydrogen molecules are formed

TABLE I. Dependence of the coefficients a and b from Eq. (3) on orthohydrogen concentration.

σ -H ₂ Concentration (%)	a (mW/cm ² K ⁴)	b (cm/mW)
0.20	110	1.4×10^{-4}
0.34	92	10^{-4}
0.52	61.5	10^{-4}
0.71	55.0	10^{-4}
1.1	32.9	10^{-4}
2.5	15.3	10^{-4}
5.0	4.6	10^{-4}

during crystal growth is not very much greater than would be expected statistically.

If scattering mechanisms requiring segregation of the orthohydrogen molecules are to be ruled out, we must consider the possibility that the low-temperature thermal resistivity is, in fact, due to impurity scattering. But the impurity scattering cannot be of the kind usually associated with point defects. It must depend on some mode of interaction between phonons and orthohydrogen molecules that is much less frequency dependent than pure Rayleigh scattering.

The phonon-orthohydrogen interaction is studied in some detail in Ref. 2. The calculation of phonon scattering rates presented there includes the contribution made by excitation of the orthohydrogen molecule's internal energy levels and the effects on the energy-level structure of the electric quadrupole-quadrupole interaction between orthohydrogen molecules. With this calculation, some progress seems to have been made towards an understanding of the low-temperature conductivity data. A strong dependence on both temperature and concentration is predicted for the phonon-orthohydrogen scattering rate, with the result that $K \sim T^2 x^{-2}$ for orthohydrogen concentrations $x < 10\%$. It is expected, of course, that at very low concentrations ($x < 1\%$) the effects of phonon-orthohydrogen scattering will become negligible and a concentration-independent conductivity $K \sim T^3$ will be observed. As we have remarked, the measurements show a conductivity more nearly proportional to T^3 at all concentrations. The observed concentration dependence, on the other hand, seems to be accounted for quite well by the calculation of Ref. 2. This is illustrated in Fig. 5, which shows that the prediction of a concentration dependence approaching $K \sim x^{-2}$ at sufficiently large concentrations ($x > 1\%$) is entirely consistent with the data. The regular departure of the low-temperature data points from the theoretical curves of Fig. 5 is primarily due to the difference between the calculated (T^2) and observed (T^3) temperature dependence.

Perhaps the least satisfactory aspect of this comparison is its rather qualitative nature. The final stage of the calculation reported in Ref. 2 includes the use of an adjustable parameter in the phonon-orthohydrogen scattering term to provide the "best over-all fit" to the data at all orthohydrogen concentrations. The size of this scaling factor ($A_s = 10$) suggests either that the effect of the quadrupole-quadrupole interaction has been underestimated by an order of magnitude, or that the low-temperature conductivity is governed by some other concentration-dependent scattering mechanism not yet identified. In either case the relative importance of the "static" part of the im-

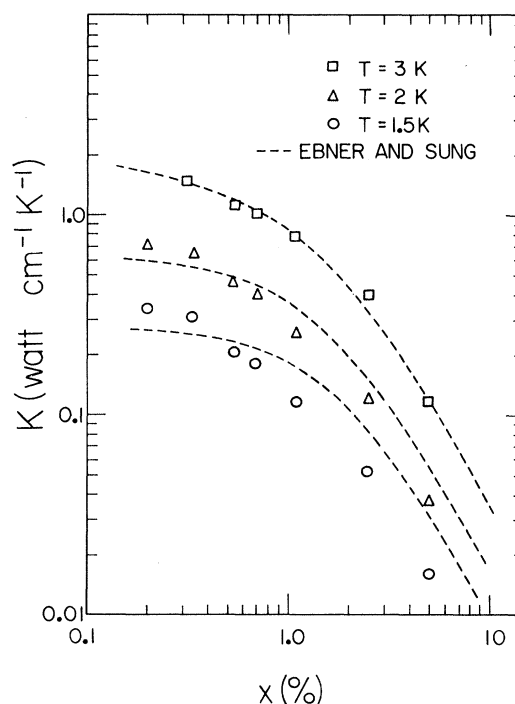


FIG. 5. Comparison of observed concentration dependence of the thermal conductivity with that calculated from Ref. 2.

purity-scattering term will have been overemphasized, since it is multiplied by the same scaling factor. This may be why the calculated conductivity shows a concentration-dependent (static) impurity scattering, while the measurements do not.

Further experiments are planned to include measurements on HD and D₂, as well as H₂. There is an evident possibility that the crystal growing technique we have described may not always yield single crystals. For this reason we regard it as highly desirable that the cryostat should be modified to permit inspection of the part of the sample actually used for the conductivity measurements, so that the birefringence of the hcp solid can be used to identify polycrystalline samples or to determine the orientation of single crystals.

ACKNOWLEDGMENTS

We acknowledge many helpful discussions with Dr. C. Ebner and Dr. C. C. Sung. We are indebted to Dr. J. Constable for measurements of the orthohydrogen concentrations. It is a particular pleasure to acknowledge the encouragement given this work by Dr. J. R. Gaines, who also provided the hydrogen-gas samples.

*Work supported in part by the U.S. Air Force Office of Scientific Research, under Contract No. AF-AFOSR-1273-67.

†Present address: Dept. of Physics and Astronomy, U. of Toledo, Toledo, Ohio 43606.

¹R. W. Hill and B. Schneidmeyer, *Z. Physik Chem. Neue Folge*, Bd. 16, 257 S (1958).

²C. Ebner and C. C. Sung, preceding paper, *Phys. Rev. B* 2, 2115 (1970).

³W. Hardy and J. R. Gaines, *Phys. Rev. Letters* 17, 1278 (1966).

⁴NBS Monograph No. 10 (USGPO, Washington, D. C.,

1960).

⁵H. Fritzsche, *Phys. Rev.* 99, 406 (1955).

⁶P. Lindenfeld, *Rev. Sci. Instr.* 32, 9 (1961).

⁷R. W. Hill and O. V. Lounasmaa, *Phil. Mag.* 4, 785 (1959).

⁸J. Jarvis, D. Ramm, and H. Meyer, *Phys. Rev. Letters* 18, 119 (1967).

⁹A. B. Harris, L. I. Amstutz, H. Meyer, and S. M. Meyers, *Phys. Rev.* 175, 603 (1968).

¹⁰L. I. Amstutz, J. R. Thompson, and H. Meyer, *Phys. Rev. Letters* 21, 1175 (1968).

Extreme-Ultraviolet Spectra of Ionic Crystals*

Frederick C. Brown, Christian Gähwiler, Hiizu Fujita, †

A. Barry Kunz, William Scheifley, ‡ and Nicholas Carrera ‡

Department of Physics and Materials Research Laboratory University of Illinois, Urbana, Illinois 61801

(Received 1 April 1970)

The absorption spectra of several ionic crystals were obtained by the use of synchrotron radiation with photon energies in the range 50–250 eV. This range includes thresholds for excitation of both p and d core states. Arguments are given that peaks in the observed spectra are generally due to maxima in the final density of states, rather than exciton phenomena. The chlorine $L_{II,III}$ spectra of NaCl, KCl, RbCl, and even AgCl are very much alike, which can be understood in terms of similar conduction-band structure for these materials. It is suggested that double excitations are not as important as collective effects. The $3d \rightarrow p$ spectra of the Br⁻ Kr-Rb⁺ sequence, as well as the $4d \rightarrow p$ spectra of the I⁻-Xe-Cs⁺ sequence, can be understood by taking into account the spin-orbit splitting of the initial states and the final-state band structure. Very prominent d -to- f resonances were found for compounds containing iodine and cesium. In CsCl and CsBr, structure near 160 eV due to excitation of the cesium N_{III} level shows an unusual antiresonance behavior.

I. INTRODUCTION

Our present knowledge of the optical constants of solids for photon energies in the range 20–200 eV is relatively incomplete. Until recently very few continuum light sources were available for high-resolution spectroscopy in the region of grazing incidence optics, say from 50 to 500 Å. Also it has been generally thought that well-defined or characteristic structure is absent in this high-energy region due to the exhaustion of oscillator strength as well as severe lifetime broadening. Actually, a great deal of structure does exist, and our knowledge of the spectral detail is rapidly being improved through the use of synchrotron radiation. Especially strong efforts are under way at the German electron synchrotron (DESY) in Hamburg and at the Tokyo synchrotron by the INSOR (Institute for Nuclear Studies – Synchrotron Orbital Radiation) group. In the present paper we present results obtained on a variety of alkali halides at the 250-MeV electron storage ring¹ of the University of Wisconsin Physical Science Laboratory in Stoughton, Wisc.

The spectra presented below are the result of largely exploratory observations carried out on specific sequences of elements in ionic crystals. In general, we would like to know how better to relate optical response and band structure. It is well known that density-of-states and matrix elements are important in optical transitions. This leads us to ask the question: Is it possible to confirm the essential features of recent band calculations on ionic crystals^{2–6} by exciting electrons from narrow bands of core states of various symmetry – for example, from s , p , or d levels? On the other hand, what new processes perhaps of a collective nature have to be introduced in order to explain the high-energy optical properties of a solid? How is the situation different in a gas compared to a solid? Are antiresonances due to configuration interactions observable in solid-state spectra as well as for autoionizing transitions of gases?⁷ Are excitons actually produced for energies which overlie the continuum, and if so, how important are multiple exciton processes?^{8,9}

After a brief description of the experimental